

# The Instability of Flow Through a Slowly Diverging Pipe With Viscous Heating

Kirti Chandra Sahu

Department of Chemical Engineering,  
Indian Institute of Technology Hyderabad,  
Yeddumailaram 502 205,  
Andhra Pradesh, India  
e-mail: ksahu@iith.ac.in

*The nonparallel linear stability analysis of flow through a slowly diverging pipe undergoing viscous heating is considered. The pipe wall is maintained at constant temperatures and Nahme's law is applied to model the temperature dependence of the fluid viscosity. A one-parameter family of velocity profiles for the basic state is obtained for small angles of divergence. The nonparallel stability equations for the disturbance velocity coupled to a linearized energy equation are derived and solved using a spectral collocation method. Our results indicate that increasing viscous heating, characterized by increasing Nahme number, is destabilizing. The Prandtl number has a negligible effect on the linear stability characteristics. The Grashof number stabilizes the flow for  $Gr > 10^6$ , below which it has a negligible effect. [DOI: 10.1115/1.4004299]*

## 1 Introduction

The dynamics of fluid flows with temperature-dependent properties have been the subject of numerous experimental, theoretical, and numerical studies due to their relevance to practical applications; these include lubrication, tribology, food processing, instrumentation, and viscometry. In polymer processing industries [1], viscous heating plays an important role as many fluids in such applications strongly depend on temperature.

In Couette and Taylor-Couette flows the effect of viscous heating has been studied by many researchers via linear stability analysis [2–4] and experimental observation [5]. These systems are widely studied as the Couette and Taylor-Couette (with fixed inner cylinder) flows are always stable to small disturbances. They found that the “critical” Reynolds number (the minimum Reynolds number at which the flow is linearly unstable) decreases as the viscous heating increases. This effect was attributed to the coupling between the velocity perturbations and the base state temperature gradient. Pinarbasi et al. [6] showed that viscous heating destabilizes the inelastic fluid flow through a symmetrically heated channel. Costa et al. [7] studied the effect of viscous heating with temperature-dependent viscosity in a symmetrically heated channel flow via linear stability analysis and direct numerical simulations. They found that viscous heating can trigger and sustain secondary rotational flows. Recently, Sahu et al. [8] performed a linear stability analysis to study the effects of viscous heating on Poiseuille flow in an asymmetrically heated channel and found that viscous heating has a destabilizing influence.

The flow through spatially varying geometries, such as, diverging, converging-diverging channels/pipes are common in oil-gas, paint, chemical, and polymer industries, where viscous heating also plays an important role. Isothermal flows through various spatially varying geometries have been studied by many researchers [9–13]. Floryan et al. [10] studied the behavior of the traveling wave disturbances in a converging-diverging channel via a temporal linear stability analysis. They have shown that the variations in the channel geometry destabilize the flow, as compared with the straight channel case. A global stability analysis of the flow through a diverging channel was recently conducted by Swaminathan et al. [9]. They found the instability characterized by the “global” mode obtained from this analysis is qualitatively differ-

ent from that obtained by parallel and weakly nonparallel approaches. Selvarajan et al. [13] studied the linear stability characteristics of a symmetric wavy walled channel flow. They showed that the fastest growing unstable mode arises due to the waviness of the walls. One particular interest is the work of Sahu et al. [11] who investigated the linear instability of isothermal flow through a slowly diverging pipe. They found that the critical Reynolds number for linear instability of the laminar flow through a diverging pipe is finite, and approaches infinity as the inverse of the divergence angle. An experimental confirmation of this result has recently been obtained by Peixinho [14]. As the above brief review shows, in spite of the number of works carried out in isothermal flow through spatially varying geometries, the effect of wall's temperature and viscous heating have received far less attention irrespective of the importance of viscous heating effect in many industrial applications. In the present paper the effect of viscous heating on the linear instability of flow through a slowly diverging pipe is studied. As discussed above, like Couette and Taylor-Couette flows, the Hagen-Poiseuille flow is also a system where the flow is linearly stable to any small disturbance. Thus it is fundamentally interesting to study the effect of viscous heating in this system. The effects of viscous heating in Hagen-Poiseuille flow is studied as a special case that can be achieved by setting angle of divergence to zero in the present formulation.

The rest of this paper is organized as follows. Details of the problem formulation are provided in Sec. 2, and the results of the linear stability analysis are presented in Sec. 3. Concluding remarks are provided in Sec. 4.

## 2 Formulation

A pressure-driven flow of an incompressible and Newtonian fluid through a slowly diverging pipe undergoing viscous heating is considered. A cylindrical coordinate system  $(x, r, \theta)$  is used to model this flow, where  $x$ ,  $r$ , and  $\theta$  denote the axial, radial, and azimuthal coordinates, respectively. The rigid and impermeable pipe wall is maintained at a constant temperature  $T_w$ . In the literature the effect of viscous heating has been studied using either Arrhenius-type relationships [15,16] or a Nahme-type law [2,4,6,17,18] to model the temperature-viscosity relationship. In the present study the following Nahme-type viscosity-temperature relationship [19] is used that approximates the variation of viscosity of many liquids over a wide range of temperature  $T$ . A similar viscosity-temperature relationship was previously used by several authors [2,19,20]

Contributed by the Fluids Engineering Division of ASME for publication in the JOURNAL OF FLUIDS ENGINEERING. Manuscript received October 31, 2010; final manuscript received May 19, 2011; published online July 5, 2011. Assoc. Editor: Ye Zhou.

$$\mu(T) = \mu_{ref} \exp \left[ -\beta \frac{(T - T_{ref})}{T_{ref}} \right] \quad (1)$$

where  $\beta$  is a dimensionless activation energy parameter which characterizes the sensitivity of the viscosity to the temperature variation; for liquids,  $\beta$  is a positive number, and we restrict ourselves to this case;  $\mu_{ref}$  is the dynamic viscosity of the fluid at the inlet of the pipe at  $T_{ref} (\equiv 25^\circ\text{C})$ .

**2.1 The Basic Flow.** Near-similar equations of one-parameter family of velocity and temperature profiles for the basic state is derived at small angle of divergence, where the parameter

$$S \equiv a\text{Re} \quad (2)$$

varies slowly in the axial coordinate  $x$ . Here  $\text{Re} = U_c(x) \rho R(x) / \mu_{ref}$  is the Reynolds number and  $a (\equiv (dR(x)/dx) \ll 1)$  is the slope of the pipe, wherein  $R(x)$ ,  $U_c(x)$  and  $\rho$  denote the local radius, local centerline velocity, and density of the fluid, respectively. The basic state is assumed to be axisymmetric and the temperature is fully developed. Thus we neglect variation of temperature in the axial direction. The steady, axisymmetric momentum and energy equations are given by

$$\rho \left[ U \frac{\partial U}{\partial x} + V \frac{\partial U}{\partial r} \right] = -\frac{\partial P}{\partial x} + \frac{\mu_0}{r} \left[ \frac{\partial V}{\partial x} + \frac{\partial U}{\partial r} \right] + \frac{\partial}{\partial r} \left[ \mu_0 \left( \frac{\partial V}{\partial x} + \frac{\partial U}{\partial r} \right) \right] + \frac{\partial}{\partial x} \left[ 2\mu_0 \frac{\partial U}{\partial x} \right] \quad (3)$$

$$\rho \left[ U \frac{\partial V}{\partial x} + V \frac{\partial V}{\partial r} \right] = -\frac{\partial P}{\partial r} + \frac{1}{r} \left[ 2\mu_0 \frac{\partial V}{\partial r} \right] + \frac{\partial}{\partial r} \left[ 2\mu_0 \frac{\partial V}{\partial r} \right] + \frac{\partial}{\partial x} \left[ \mu_0 \left( \frac{\partial V}{\partial x} + \frac{\partial U}{\partial r} \right) \right] \quad (4)$$

$$\rho c_p \left[ U \frac{\partial T_0}{\partial x} + V \frac{\partial T_0}{\partial r} \right] = \kappa \left[ \frac{1}{r} \frac{\partial}{\partial r} \left( r \frac{\partial T_0}{\partial r} \right) + \frac{\partial^2 T_0}{\partial x^2} \right] + \mu_0 \left[ 2 \left\{ \left( \frac{\partial U}{\partial x} \right)^2 + \left( \frac{\partial V}{\partial r} \right)^2 + \left( \frac{V}{r} \right)^2 \right\} + \left( \frac{\partial V}{\partial x} + \frac{\partial U}{\partial r} \right)^2 \right] \quad (5)$$

where  $\mu_0$ ,  $c_p$ ,  $T_0$ ,  $U$ , and  $V$  represent the dynamic viscosity, specific heat capacity at constant pressure, temperature, axial, and radial velocity components for the basic state, respectively. Eliminating pressure  $P$  from Eqs. (3) and (4) and neglecting the higher order terms, we obtain

$$\rho \left[ -\frac{V}{r} \frac{\partial U}{\partial r} + U \frac{\partial^2 U}{\partial x \partial r} + V \frac{\partial^2 U}{\partial r^2} \right] = \frac{\mu_0}{r} \frac{\partial^2 U}{\partial r^2} - \frac{\mu_0}{r^2} \frac{\partial U}{\partial r} + \frac{1}{r} \frac{\partial \mu_0}{\partial r} \frac{\partial U}{\partial r} + \frac{\partial^2 \mu_0}{\partial r^2} \frac{\partial U}{\partial r} + 2 \frac{\partial \mu_0}{\partial r} \frac{\partial^2 U}{\partial r^2} + \mu_0 \frac{\partial^3 U}{\partial r^3} \quad (6)$$

The velocity components are then re-expressed in terms of the stream function  $\Psi$  as

$$(U, V) = \left( \frac{1}{r} \frac{\partial \Psi}{\partial r}, -\frac{1}{r} \frac{\partial \Psi}{\partial x} \right)$$

to satisfy the continuity equation. Substituting the above expressions of  $U$  and  $V$  in Eq. (6), we obtain

$$\rho \left[ -3 \frac{\partial \Psi}{\partial x} \frac{\partial \Psi}{\partial r} + 3r \frac{\partial \Psi}{\partial x} \frac{\partial^2 \Psi}{\partial r^2} - r \frac{\partial \Psi}{\partial r} \frac{\partial^2 \Psi}{\partial x \partial r} + r^2 \frac{\partial \Psi}{\partial r} \frac{\partial^3 \Psi}{\partial x \partial r^2} - r^2 \frac{\partial \Psi}{\partial x} \frac{\partial^3 \Psi}{\partial r^3} \right] = r^3 \mu_0 \frac{\partial^4 \Psi}{\partial r^4} - 2r^2 \mu_0 \frac{\partial^3 \Psi}{\partial r^3} + 3r \mu_0 \frac{\partial^2 \Psi}{\partial r^2} - 3\mu_0 \frac{\partial \Psi}{\partial r} + 3r \frac{\partial \mu_0}{\partial r} \frac{\partial \Psi}{\partial r} - 3r^2 \frac{\partial \mu_0}{\partial r} \frac{\partial^2 \Psi}{\partial r^2} + 2r^3 \frac{\partial \mu_0}{\partial r} \frac{\partial^3 \Psi}{\partial r^3} - r^2 \frac{\partial^2 \mu_0}{\partial r^2} \frac{\partial \Psi}{\partial r} + r^3 \frac{\partial^2 \mu_0}{\partial r^2} \frac{\partial^2 \Psi}{\partial r^2} \quad (7)$$

The following scaling is employed in order to render Eq. (7) dimensionless:

$$r = R\tilde{r}, \Psi = U_c R^2 \tilde{\Psi}, (U, V) = U_c (\tilde{U}, \tilde{V}), dx = R\tilde{d}x, \mu_0(T_0) = \tilde{\mu}_0(T_0) \mu_{ref} \quad (8)$$

where the tildes designate dimensionless quantities. The Reynolds number is assumed to be high and the angle of divergence is small enough, such that, all terms of order  $O(\text{Re}^{-2})$  or  $O(a^2)$  and higher are negligible. After dropping tildes from all nondimensional terms, the resultant equation in the dimensionless form becomes

$$\left( q\Psi - ar\Psi' \right) \left( -3\Psi' + 3r\Psi'' - r^2\Psi''' \right) - r\Psi' \left( q\Psi' + ar\Psi'' - a\Psi' \right) + r^2\Psi' \left( q\Psi'' - 2a\Psi''' - ar\Psi'''' \right) = \frac{1}{\text{Re}} \left[ r^3\mu_0\Psi'''' - 2r^2\mu_0\Psi'''' + 3r\mu_0\Psi'''' - 3\mu_0\Psi'''' + 3r\mu_0'\Psi'' - 3r^2\mu_0'\Psi'' + 3r^3\mu_0'\Psi'' - r^2\mu_0''\Psi' + r^3\mu_0''\Psi' \right] \quad (9)$$

where primes denote differentiation with respect to  $r$  and  $q \equiv (1/U_c R^2) d/dx (U_c R^2)$ . For near-similar flow, imposing constant mass flow rate condition (setting  $q=0$ ), we obtain

$$\mu_0 r^2 U'''' = -r\mu_0 U'' + \mu_0 U' - 4Sr^2 U U' - 3r\mu_0' U' - 3r^2 \mu_0' U'' - r^2 \mu_0'' U' \quad (10)$$

$$V = arU \quad (11)$$

Similarly, neglecting the higher order terms, after nondimensionalizing the energy equation by employing

$$T_0 = \frac{T_{ref} \tilde{T}_0}{\beta} + T_{ref} \quad (12)$$

and then dropping tildes from all nondimensional terms, yields

$$T_0'' + \frac{T_0'}{r} + \text{Na} \mu_0 (U')^2 = 0 \quad (13)$$

where  $\text{Na} (\equiv \beta \mu_{ref} U_c^2 / \kappa T_{ref})$  is the Nahme number and  $\kappa$  is the coefficient of thermal conductivity. It is confirmed that for isothermal flow, Eq. (10) reduces to the axisymmetric Jeffery-Hamel equation [11].

The dimensionless viscosity-temperature relationship for the basic state is given by

$$\mu_0(T_0) = \exp(-T_0) \quad (14)$$

The coupled Eqs. (10), (11), and (13) are solved using a fourth-order Runge-Kutta method with the following boundary conditions:

$$U = 0, \text{ and } T_0 = r_T \text{ at } r = 1 \quad (15)$$

$$U = 1, U' = 0 \text{ and } T_0' = 0 \text{ at } r = 0 \quad (16)$$

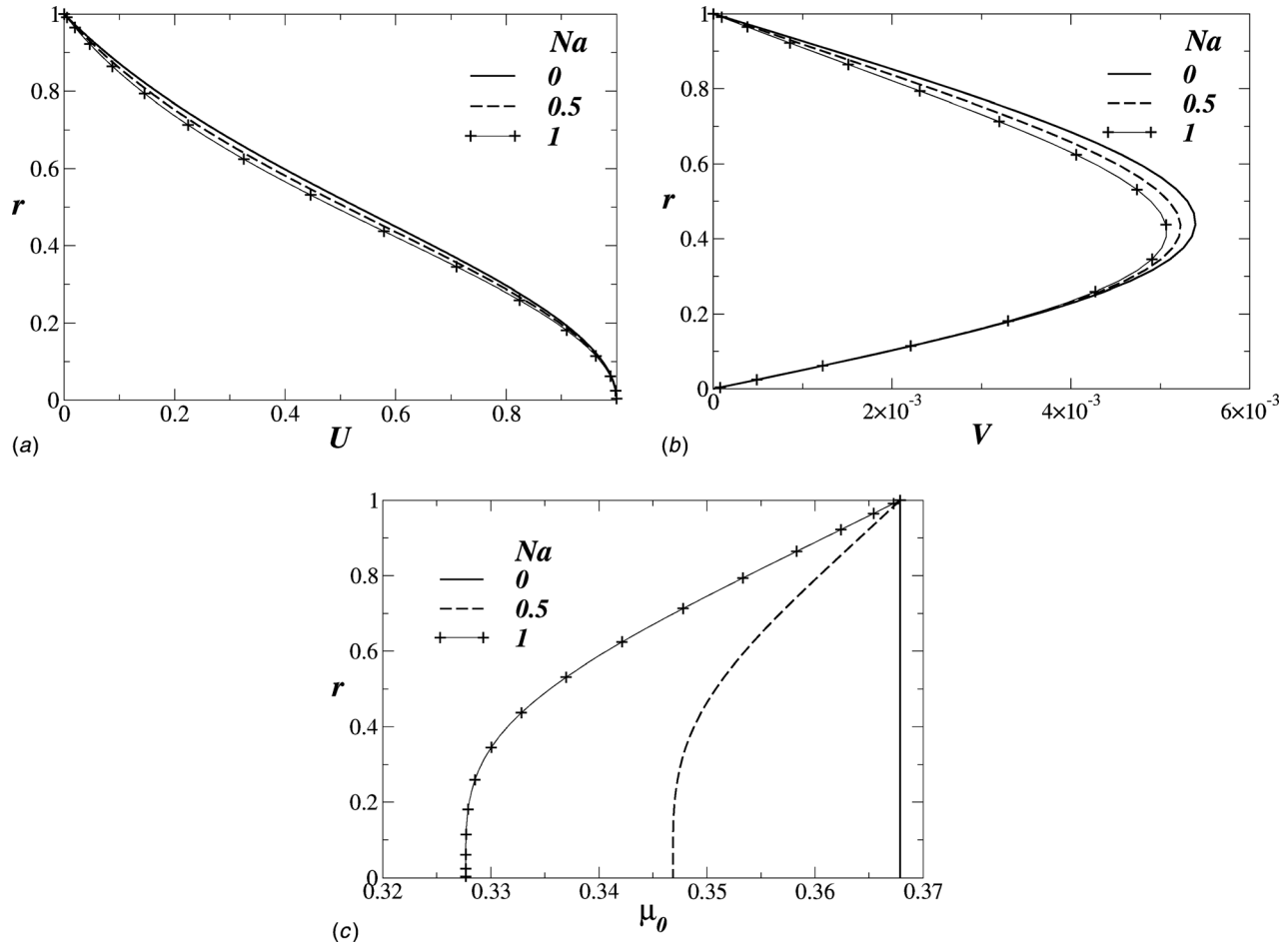


**Fig. 1 Typical basic state profiles of the axial velocity ( $U$ ), wall-normal velocity ( $V$ ) and viscosity ( $\mu_0$ ) for different  $Na$  values. The rest of the parameter values are  $Re = 100$ ,  $a = 0.02$  and  $r_T = 1$ .**

where  $r_T = \beta(T_w - T_{ref})/T_w$ . Typical basic state profiles of the axial velocity ( $U$ ), wall-normal velocity ( $V$ ) and viscosity ( $\mu_0$ ) for different values of  $Na$  are shown in Fig. 1. The rest of the parameter values are  $Re = 100$ ,  $a = 0.02$  and  $r_T = 1$ . Inspection of Fig. 1(a) reveals that the tendency of the profiles to become inflectional ( $U'' = 0$  in the velocity profile) increases with increase in  $Na$ . It can also be seen that the wall-normal velocity and viscosity decrease with increase in  $Na$ ; it is found that point of inflection (not shown) always lies near the wall. These features indicate that increasing  $Na$  is expected to exert a destabilizing influence on the flow [21].

**2.2 Nonparallel Stability Analysis.** The temporal linear stability of the base state obtained by solving Eqs. (10), (11), and (13) to infinitesimal, three-dimensional (3D) disturbances is examined. Since the flow under consideration varies significantly in the axial direction a normal mode form can only be used in the time and azimuthal directions. The perturbation in the axial direction can be expressed as a rapidly varying wavelike part scaled by a relatively slowly varying function [11,22], such as

$$(u, v, w, p, T, \mu)(x, r, \theta, t) = [U(x, r), V(x, r), 0, P(x, r), T_0(x, r), \mu_0(x, r)] + \text{Real} \left\{ \left[ \hat{u}(x, r), \hat{v}(x, r), \hat{p}(x, r), \hat{T}(x, r), \hat{\mu}(x, r) \right] \times \exp \left[ \mathbf{i} \left( \int \alpha(x) dx + n\theta - \Omega t \right) \right] \right\} \quad (17)$$

where the quantities  $\hat{u}$ ,  $\hat{v}$  and  $\hat{w}$  are the amplitudes of the axial, radial, and azimuthal components of perturbation velocity, respectively;  $\hat{p}$  and  $\hat{T}$  denote the amplitude of the perturbation pressure and temperature, respectively;  $\alpha(x)$  is the dimensionless axial wave number (real);  $n$  is the number of wave in the azimuthal direction;  $\Omega (= \alpha c)$  and  $c$  are the complex frequency and the phase speed of the disturbance, respectively. Here  $i = \sqrt{-1}$  and  $\hat{\mu} = (d\mu_0/dT_0)\hat{T}$  represents the amplitude of the perturbation viscosity. Substitution of Eq. (17) into the Navier-Stokes and continuity equations in cylindrical coordinate [23] followed by subtraction of the base state equations, subsequent linearization and neglecting higher order terms  $O(Re^{-2})$  [ $O(Re^{-2})$  or  $O(a^2)$  and higher] yields the following coupled partial differential equations for the perturbation quantities (following the suppression of the hat decoration)

$$\begin{aligned} -i\Omega u + U \left( 2 \frac{U'}{U_c} u + \frac{\partial u}{\partial x} + \alpha u - ar \frac{\partial u}{\partial r} \right) + u \left( \frac{\partial U}{\partial x} - ar \frac{\partial U}{\partial r} \right) \\ + V \frac{\partial u}{\partial r} + v \frac{\partial U}{\partial r} = -2 \frac{U'}{U_c} p - \frac{\partial p}{\partial x} - \alpha p + ar \frac{\partial p}{\partial r} \\ + \frac{\mu_0}{Re} \left[ \frac{\partial^2 u}{\partial r^2} + \frac{1}{r} \frac{\partial u}{\partial r} - \left( \frac{n^2}{r^2} + \alpha^2 \right) u \right] + \frac{1}{Re} \frac{\partial \mu_0}{\partial r} \left( \frac{\partial u}{\partial r} + \alpha v \right) \\ + \frac{\mu}{Re} \left( \frac{\partial^2 U}{\partial r^2} + \frac{1}{r} \frac{\partial U}{\partial r} \right) + \frac{1}{Re} \frac{\partial \mu}{\partial r} \frac{\partial U}{\partial r} \end{aligned} \quad (18)$$

$$\begin{aligned}
& -i\Omega v + U \left( \frac{U'_c}{U_c} v + \frac{\partial v}{\partial x} + i\alpha v - ar \frac{\partial v}{\partial r} \right) + V \frac{\partial v}{\partial r} + v \frac{\partial V}{\partial r} \\
& = -\frac{\partial p}{\partial r} + \frac{\mu_0}{\text{Re}} \left[ \frac{\partial^2 v}{\partial r^2} + \frac{1}{r} \frac{\partial v}{\partial r} - \frac{(1+n^2)}{r^2} v - \frac{2in}{r^2} w - \alpha^2 v \right] \\
& + \frac{2}{\text{Re}} \frac{\partial \mu_0}{\partial r} \frac{\partial v}{\partial r} + \frac{i\alpha \mu_0}{\text{Re}} \frac{\partial U}{\partial r} - \frac{\text{Gr}}{\text{Re}^2} T
\end{aligned} \quad (19)$$

$$\begin{aligned}
& -i\Omega w + U \left( \frac{U'_c}{U_c} w + \frac{\partial w}{\partial x} + i\alpha w - ar \frac{\partial w}{\partial r} \right) + V \frac{\partial w}{\partial r} + \frac{Vw}{r} \\
& = -\frac{in}{r} p + \frac{\mu_0}{\text{Re}} \left[ \frac{\partial^2 w}{\partial r^2} + \frac{1}{r} \frac{\partial w}{\partial r} - \frac{(1+n^2)}{r^2} w - \frac{2in}{r^2} v - \alpha^2 w \right] \\
& + \frac{1}{\text{Re}} \frac{\partial \mu_0}{\partial r} \left( \frac{\partial w}{\partial r} - \frac{w}{r} + \frac{inw}{r} \right)
\end{aligned} \quad (20)$$

$$\frac{\partial v}{\partial r} + \frac{v}{r} + \frac{inw}{r} + \frac{U'_c}{U_c} u + \frac{\partial u}{\partial r} + i\alpha u - ar \frac{\partial u}{\partial r} = 0 \quad (21)$$

$$\begin{aligned}
& -i\Omega T + U \left( \frac{\partial T}{\partial x} + i\alpha T - ar \frac{\partial T}{\partial r} \right) + u \left( \frac{\partial T_0}{\partial x} - ar \frac{\partial T_0}{\partial r} \right) + V \frac{\partial T}{\partial r} + v \frac{\partial T_0}{\partial r} \\
& = \frac{1}{\text{RePr}} \left[ \frac{\partial^2 T}{\partial r^2} + \frac{1}{r} \frac{\partial T}{\partial r} - \left( \frac{n^2}{r^2} + a^2 \right) T \right] + \mu \frac{\text{Na}}{\text{RePr}} \left( \frac{\partial U}{\partial r} \right)^2
\end{aligned} \quad (22)$$

Here  $U'_c = dU_c/dx$ .  $\text{Gr} (\equiv \alpha_0 T_w g R^3 / \beta \mu_{ref}^2)$  and  $\text{Pr} (\equiv c_p \mu_{ref} / \kappa)$  are the Grashof and Prandtl numbers, respectively, wherein  $\alpha_0$  is the thermal expansion coefficient and  $\mathbf{g}$  is the acceleration due to gravity. It can be seen that these equations are coupled and the extent of coupling increases with  $\text{Na}$ . Eqs. (18)–(22) may be rewritten in the form

$$\mathcal{H}\phi(x, r) + \mathcal{G} \frac{\partial \phi(x, r)}{\partial x} = \Omega \mathcal{B}\phi(x, r), \quad (23)$$

where  $\phi \equiv [u, v, w, p, T]$  is eigenfunction. Note that a given mode is unstable if  $\Omega_i > 0$ , stable if  $\Omega_i < 0$  and neutrally stable if  $\Omega_i = 0$ ; where  $\Omega_i$  the imaginary part of the perturbation frequency. The minimum Reynolds number in the neutral stability curve (contour of  $\Omega_i = 0$  in  $\alpha$  against  $\text{Re}$  plot) is referred to as a “critical” Reynolds number,  $\text{Re}_{cr}$ . In the limit  $(\text{Na}, \text{Gr}, a, U'_c, \partial \phi / \partial x) \rightarrow 0$ , these equations reduce to those of Gill [24] and Lessen et al. [25] for the parallel (fully developed) flow through a straight pipe. In the limit  $(\beta, \text{Na}, \text{Gr}) \rightarrow 0$ , we can also recover the nonparallel stability equations of Sahu et al. [11] for isothermal flow through a slowly diverging pipe.

The boundary conditions are obtained from no-slip and no-penetration conditions at the pipe wall and by demanding that all components of the velocity perturbation vary continuously with  $r$  at the centerline [26]; the values of perturbation temperature at the wall and centerline are zero.

$$u = v = w = p = T = 0, \text{ at } r = 0, \text{ for } n \neq 1 \quad (24)$$

$$u = p = 0, v + iw = 0, \text{ at } r = 0, \text{ for } n = 1 \quad (25)$$

$$u = v = w = T = 0, \text{ at } r = 1 \quad (26)$$

Note that for  $n=1$ , we have seven boundary conditions for an eighth order differential system of equations. Thus an extra boundary condition is generated by differentiating the continuity equation with respect to  $r$ , and using the no-slip boundary condition at the wall.

$$2 \frac{\partial v}{\partial r} + in \frac{\partial w}{\partial r} = 0 \text{ at } r = 0 \quad (27)$$

**2.3 Numerical Procedure and Validation.** A similar procedure as that of Sahu et al. [11] is followed in order to write Eq.

(23) as an eigenvalue problem of larger size. Considering two axial locations 1 and 2 separated by an incremental distance, i.e.,  $x_2 = x_1 + \Delta x$ , we can write

$$\frac{\partial \phi}{\partial x} = \frac{(\phi_2 - \phi_1)}{\Delta x} + O(\Delta x) \quad (28)$$

Higher-order approximations to the streamwise derivative could be considered instead of Eq. (28) and the resulting eigenvalue system would be of correspondingly large size. Since the dimensional frequency of the disturbance remains constant as we move downstream,  $\Omega_1$  and  $\Omega_2$  are related as follows

$$\kappa \equiv \frac{\Omega_2}{\Omega_1} = (1 + a\Delta x) \frac{U_{c1}}{U_{c2}} \quad (29)$$

Now Eq. (23) can be rewritten as an eigenvalue problem of larger size [11]

$$\begin{bmatrix} \mathcal{H}_1 - \mathcal{G}_1/\Delta x & \mathcal{G}_1/\Delta x \\ -\mathcal{G}_2/\Delta x & \mathcal{H}_2 + \mathcal{G}_2/\Delta x \end{bmatrix} \begin{bmatrix} \phi_1 \\ \phi_2 \end{bmatrix} = \Omega_1 \begin{bmatrix} \mathcal{B} & 0 \\ 0 & \kappa \mathcal{B}_2 \end{bmatrix} \begin{bmatrix} \phi_1 \\ \phi_2 \end{bmatrix} \quad (30)$$

where the subscripts 1 and 2 represent quantities at  $x_1$  and  $x_2$ , respectively. The eigenvalue  $\Omega_1$  and the eigenfunctions  $\phi_1$  and  $\phi_2$  are obtained via solution of Eqs. (30) using the Chebyshev spectral collocation method [27], accomplished by the specification of the collocation points chosen to be the Chebyshev Gauss-Lobatto points defined as  $r_j = [1 + \cos(j\pi/N)]/2$ , where  $j = (1, N)$ ,  $N$  is the order of Chebyshev polynomials.

The dependence of our numerical solutions upon mesh refinement is then investigated in Fig. 2, in which the neutral stability curves for a typical set of parameters ( $a = 0.02$ ,  $r_T = 0.5$ ,  $\text{Na} = 0.3$ ,  $\text{Gr} = 0$ ,  $\text{Pr} = 1$ , and  $n = 1$ ) are plotted. It can be seen that the curves are virtually indistinguishable for different values of  $N$ .  $\Delta x = 0.05$  is used to generate this plot; we checked that halving or doubling the value of  $\Delta x$  has even less of an effect on the eigenvalues. The results discussed in the rest of this paper are generated using  $N = 81$  and  $\Delta x = 0.05$ .

In order to validate the predictions of our numerical procedure, in Fig. 3 the eigenvalue spectrum ( $c_i$  against  $c_r$  plot) of an isothermal flow through a straight pipe obtained by solving Eq. (30) after setting  $a = 0$ ,  $\text{Na} = 0$ , and  $r_T = 0$  is compared with that of Schmid et al. [28]. It is found that every eigenvalue matches up to the 10<sup>th</sup> decimal place. As discussed latter in this paper, excellent agreements are also obtained with the results of Sahu et al. [11] for flow through a diverging pipe.

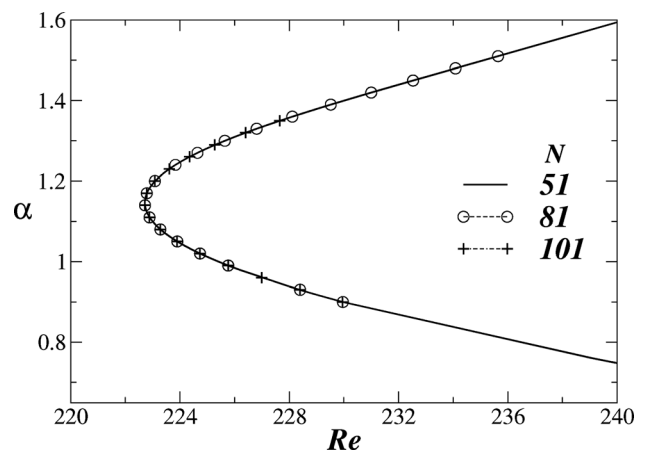


**Fig. 2** The effect of increasing the order of Chebyshev polynomials  $N$  on the neutral stability curves ( $\alpha$  versus  $\text{Re}$ ) for  $a = 0.02$ ,  $r_T = 0.5$ ,  $\text{Na} = 0.3$ ,  $\text{Gr} = 0$ ,  $\text{Pr} = 1$ , and  $n = 1$

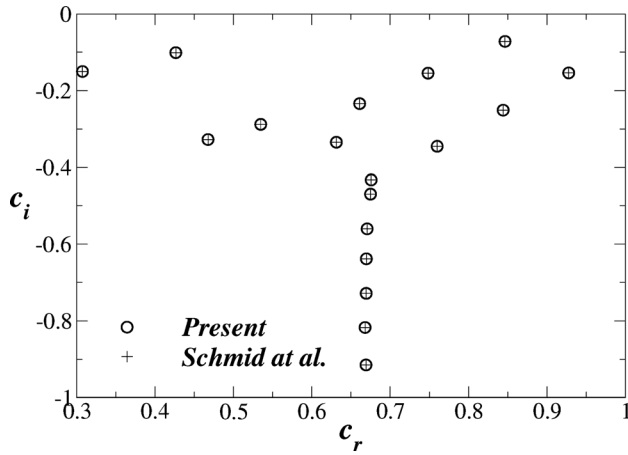


**Fig. 3 Comparison of the eigenvalue distribution generated for the isothermal, fully developed flow through a straight pipe with that of Schmid et al. [28]. The parameter values are  $Re = 2000$ ,  $a = 0$ ,  $r_T = 0$ ,  $Na = 0$ ,  $\alpha = 0.5$  and  $n = 1$ .**

### 3 Results and Discussion

It is observed that the swirl mode with azimuthal wave number  $n = 1$  is the fastest growing mode for the range of parameter val-

ues considered. A similar conclusion was also obtained by Burridge et al. [29] and Corcos et al. [30], and Sahu et al. [11] for flow through straight and diverging pipes, respectively. Thus all the results presented in this paper are for  $n = 1$ .

First, the effect of the viscous heating on the flow through a slowly diverging pipe ( $a = 10^{-3}$ ) is studied by plotting the neutral stability ( $\alpha$  against  $Re$ ) and dispersion ( $\Omega_i$  against  $\alpha$ ) curves for  $r_T = 1$ ,  $n = 1$ ,  $Gr = 0$ , and  $Pr = 1$ . The parameter values chosen are characteristic of a situation when the pipe wall is maintained at a temperature higher than that of the fluid, with a typical value of the Prandtl number. It can be seen in Fig. 4(a) that the critical Reynolds number decreases with increasing  $Na$ ; hence increasing  $Na$  destabilizes the flow. Close inspection of Fig. 4(a) also reveals that increasing  $Na$  shifts the most dangerous and “cut-off” (for which  $\Omega_i < 0$  for large  $\alpha$  values) modes towards higher wavenumbers, which is also evident in Fig. 4(b) where the dispersion curves are plotted for different values of  $Na$  for  $Re = 4000$ . It can be seen in Figs. 5(a) and 5(b) that increasing the influence of viscous heating is also destabilizing for  $r_T = -0.1$ , which corresponds to the situation when the pipe wall is maintained at a temperature lower than that of the fluid. An energy budget analysis similar to the one given in Selvam et al. [31] shows that the contribution arising from viscosity stratification in the radial direction increases with increase in  $Na$  making the flow more unstable.

Next, the variation of critical Reynolds number with slope of the pipe for different  $Na$  is investigated in Figs. 6(a) and 6(b) for

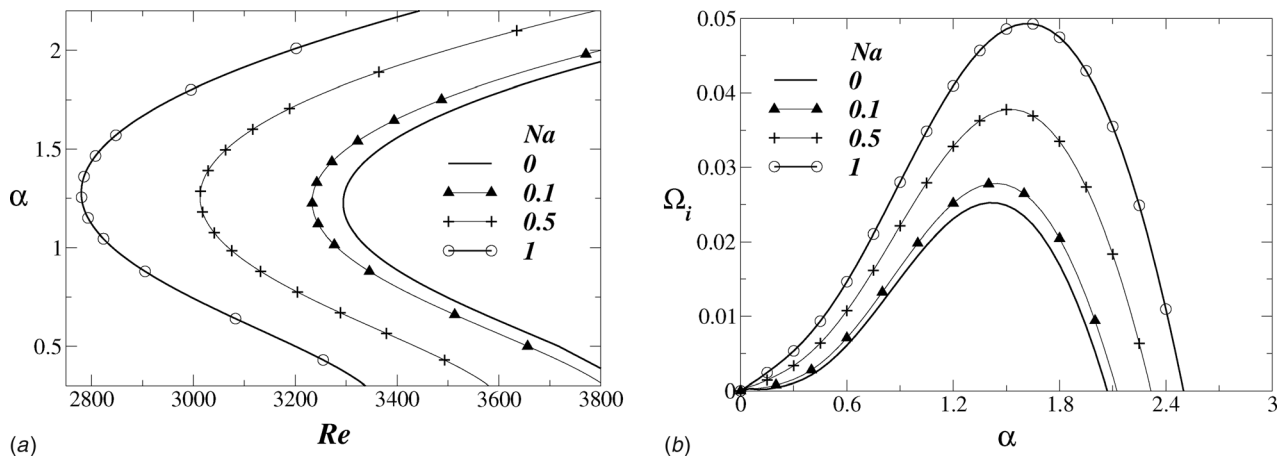


**Fig. 4 The effect of varying  $Na$  on (a) the neutral stability curves ( $\alpha$  versus  $Re$ ) and (b) dispersion curves ( $\Omega_i$  versus  $\alpha$ ) for  $r_T = 1$ . The rest of the parameter values are  $n = 1$ ,  $a = 10^{-3}$ ,  $Gr = 0$ , and  $Pr = 1$ ; a typical value of  $Re = 4000$  is considered in (b).**

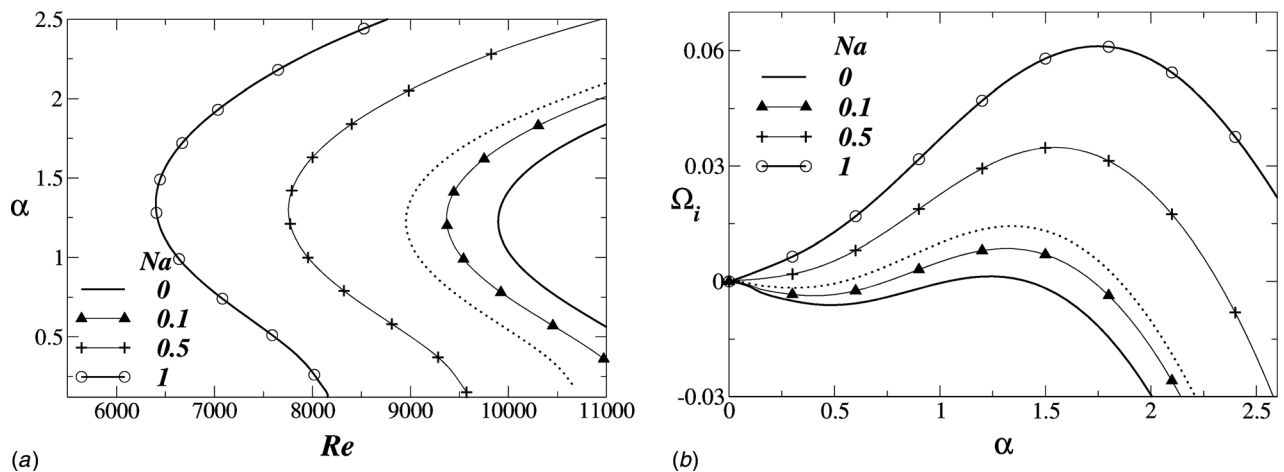


**Fig. 5 The effect of varying  $Na$  on (a) the neutral stability curves ( $\alpha$  versus  $Re$ ) and (b) dispersion curves ( $\Omega_i$  versus  $\alpha$ ) for  $r_T = -0.1$ ; a typical value of  $Re = 10^4$  is considered in (b). The rest of the parameter values are the same as those used to generate Fig. 4.**



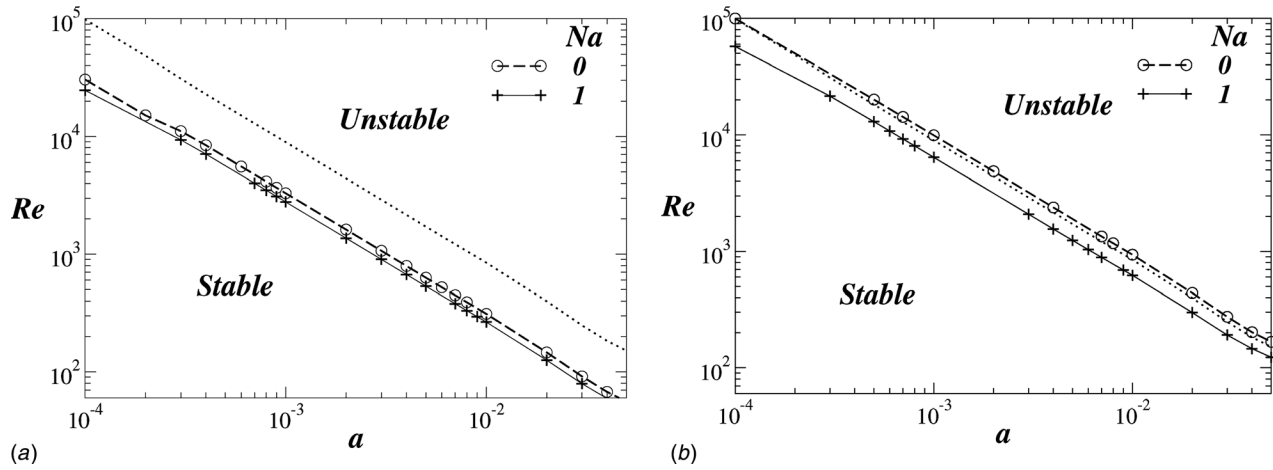


Fig. 6 Variation of critical Reynolds number with slope of the pipe  $a$  for different values of  $Na$  with (a)  $r_T = 1$  and (b)  $r_T = -0.1$ . The rest of the parameter values are  $n = 1$ ,  $Gr = 0$ , and  $Pr = 1$ . The dotted lines in (a) and (b) are associated with isothermal flow which are obtained by setting  $r_T = 0$  and  $Na = 0$ .

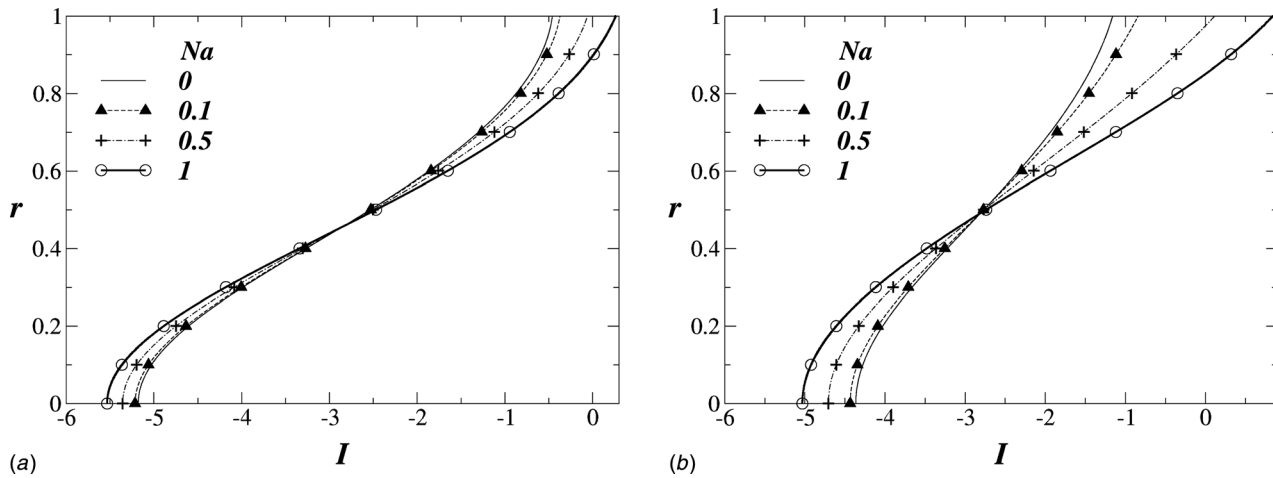


Fig. 7 Inviscid instability function  $I$  for (a)  $r_T = 1$  and (b)  $r_T = -0.1$  for different values of  $Na$ . The rest of the parameter values are  $S = 0.5$ ,  $Pr = 1$ , and  $Gr = 0$ . A typical value of  $\alpha = 1.26$  corresponding to the critical instability in Fig. 4 is used.

$r_T = 1$  and  $r_T = -0.1$ , respectively. It can be seen that power-law relationships are obeyed for different  $Na$  values. From the best fit of the data, it is found that increasing  $a$  decreases  $Re_{cr}$  as  $2.5/a$  and  $6/a$  for  $r_T = 1$  and  $r_T = -0.1$ , respectively. The critical Reynolds number varies as the inverse of the angle of divergence and approaches infinity as  $a \rightarrow 0$ . This finding indicates that the inviscid mechanism is operational. Close inspection of Fig. 6 reveals that  $Re_{cr}$  associated with  $Na = 1$  is smaller than that associated with  $Na = 0$  for all values of  $a$  considered for this set of parameters. The dotted line in Fig. 6 is for isothermal flow ( $r_T = 0$  and  $Na = 0$ ); along this line  $Re = 10/a$  [11]. This is also a validation of the present numerical procedure.

In order to understand the stability behavior, an inviscid stability analysis (outlined in the Appendix of this paper) is carried out. The necessary condition for instability in two-dimensional flow is the presence of  $U'' = 0$  in the velocity profile [32]. In Appendix it is shown that the quantity  $I \equiv U'' - (\alpha^2 r^2 - 1)/r / (\alpha^2 r^2 + 1) U'$  is the axisymmetric analog of  $U''$  in two-dimensional flow. The variation of inviscid instability function  $I$  in the radial direction is shown in Figs. 7(a) and 7(b) for  $r_T = 1$  and  $r_T = -0.1$ , respectively. The rest of the parameter values are  $S = 0.5$ ,  $Pr = 1$ ,  $Gr = 0$ , and  $\alpha = 1.26$ . The  $\alpha$  value chosen is associated with the critical instability in Fig. 4. Inspection of Figs. 7(a) and 7(b) reveals that the tendency of the profiles to have  $I = 0$  increases with  $Na$ . It can be seen that  $I$  changes sign for  $Na$  approximately

greater than 0.5, indicating that the flow is inviscidly unstable for  $Na > 0.5$  for this set of parameter values. It is also confirmed that the profiles having  $I = 0$  in Figs. 7(a) and 7(b) also satisfy

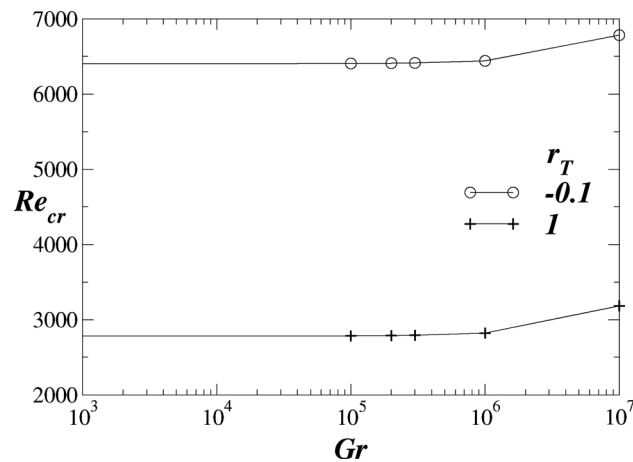


Fig. 8 The effect of  $Gr$  on the critical Reynolds number. The rest of the parameter values are  $n = 1$ ,  $a = 10^{-3}$ ,  $Na = 1$ , and  $Pr = 1$ .

Eq. (49), the additional necessary condition for the flow to be inviscidly unstable (the axisymmetric analog of the Fjørtoft's theorem in two-dimensional flow).

Finally, the effect of Grashof number  $Gr$  on the critical Reynolds number for  $r_T = 1$  and  $r_T = -0.1$  is studied in Fig. 8. Increasing  $Gr$  which is equivalent to increasing the level of buoyancy has very little effect on  $Re_{cr}$  for moderate Grashof numbers. However, at high  $Gr$  the critical Reynolds number increases slightly with increase in  $Gr$ . A similar result was also found by Sameen et al. [33] for Poiseuille flow with wall heating. It is found (not shown) that heat diffusivity, which is characterized by Prandtl number  $Pr$  has a negligible effect on the linear stability characteristics.

#### 4 Conclusion

The effect of viscous heating parameterized by a suitably defined Nahme number  $Na$  on the linear stability of the flow through a diverging pipe with a temperature-dependent viscosity is investigated. The viscosity-temperature dependence is modeled by a Nahme-type relationship. A one-parameter family of velocity profiles of the basic state is derived for small angle of divergence. The nonparallel stability equations are derived and solved as an eigenvalue problem of larger size using a spectral collocation method. After conducting a grid-independency test, the algorithm is validated by comparing of the present eigenvalue distribution with that of Schmid et al. [28] for the isothermal, fully developed flow through a straight pipe. Excellent agreement is seen for a set of typical parameters.

The present study predicts that the swirl mode is fastest growing mode, which is also known to be the critical mode in case of isothermal pipe flows. We study the effects of viscous heating by plotting the neutral stability and dispersion curves for different parameter values. Our stability results indicate that increasing viscous heating is destabilizing; the critical Reynolds number decreases with increasing  $Na$ . An inviscid analysis is carried out in order to understand the instability behavior. The instability mechanism is inviscid as the critical Reynolds number varies as the inverse of the diverging angle and approaches infinity as  $a \rightarrow 0$ . The Prandtl number has a negligible effect on the linear stability characteristics. The Grashof number stabilizes the flow for  $Gr > 10^6$ , below which it has a negligible effect.

In the future we are planning to explore the effects of viscous heating in other spatially developing geometries, such as converging-diverging pipe/channel. We are also conducting full-numerical simulations in order to understand the flow dynamics in the nonlinear regime.

#### Acknowledgment

The author would like to acknowledge the support of the Indian Institute of Technology Hyderabad, India. I thank Professor S. P. Vanka of University of Illinois at Urbana-Champaign, USA for his valuable suggestions. I also thank Dr. Parag D. Pawar for his help and encouragement.

#### Appendix: Inviscid Stability Analysis

In two-dimensional flow, the necessary conditions for instability in the inviscid limit ( $Re \rightarrow \infty$ ) have been derived by Rayleigh [32] and Fjørtoft [34], and are famously known as Rayleigh and Fjørtoft theorems, respectively. Rayleigh theorem states that it is necessary to have a point of inflection in the velocity profile for the flow to be inviscidly unstable. Fjørtoft theorem says that if a point of inflection exists, it is further necessary that  $U'''(U - U_{pi}) \leq 0$  somewhere in the profile; where  $U_{pi}$  is the velocity at the point of inflection (radial location where  $U'' = 0$ ). Here

the necessary conditions of instability for flow through a pipe in the limit  $Re \rightarrow \infty$  and  $a \rightarrow 0$  are derived. A similar analysis was also performed by Sahu et al. [35].

In the limit  $Re \rightarrow \infty$  and  $a \rightarrow 0$ , Eqs. (18)–(20) reduce to

$$-i\alpha cu + Uixu + vU' = -pi\alpha \quad (A1)$$

$$-i\alpha cv + Uixv = -p' \quad (A2)$$

$$-i\alpha cw + Uixw = -\frac{1}{r}inp \quad (A3)$$

and

$$i\alpha u + v' + \frac{v}{r} + \frac{1}{r}inw = 0 \quad (A4)$$

where  $c(= \Omega/\alpha)$  is the phase speed of the disturbance. Eliminating azimuthal velocity ( $w$ ) and pressure ( $p$ ) from the above equations, we get

$$(U - c) \left[ i\alpha u + \frac{\alpha^2 r^2}{n^2} \left( i\alpha u + v' + \frac{v}{r} \right) \right] + vU' = 0 \quad (A5)$$

$$(U - c)(i\alpha u' + \alpha^2 v) + U'ixu + v'U' + vU'' = 0 \quad (A6)$$

Differentiating Eq. (A5) with respect to  $r$  and then subtracting Eq. (A6) from the resulting equation, we obtain

$$(U - c) \left[ \frac{i\alpha r}{n^2} u' + \frac{2i\alpha}{n^2} u + \frac{3}{n^2} v' + \frac{r}{n^2} v'' + \frac{v}{r} \left( \frac{1}{n^2} - 1 \right) \right] + U' \left[ \frac{i\alpha r}{n^2} u + \frac{r}{n^2} v' + \frac{1}{n^2} v \right] = 0 \quad (A7)$$

Eliminating  $u$  and  $u'$  from the above equation by using Eqs. (A5) and (A6), we obtain

$$(U - c) \left[ v'' + \frac{(3n^2 + \alpha^2 r^2) v'}{(\alpha^2 r^2 + n^2) r} - \frac{(\alpha^2 r^2 + n^2 + 2)}{(\alpha^2 r^2 + n^2)} \alpha^2 v + (1 - n^2) \frac{v}{r^2} \right] - \left[ U'' - \frac{(\alpha^2 r^2 - n^2)}{r(\alpha^2 r^2 + n^2)} U' \right] v = 0 \quad (A8)$$

A function  $f(r)$  is defined, such that

$$\frac{f'}{f} = \left[ \frac{3n^2 + \alpha^2 r^2}{r(\alpha^2 r^2 + n^2)} \right] \quad (A9)$$

On multiplying Eq. (A8) with  $f(r)v^*$  and integrating across the pipe from  $r=0$  to  $r=1$ , we get

$$\int_0^1 (fv')' v^* dr - \int_0^1 f \left[ \frac{\alpha^2 r^2 + n^2 + 2}{\alpha^2 r^2 + n^2} \right] \alpha^2 |v|^2 dr + \int_0^1 (1 - n^2) \frac{|v|^2}{r^2} dr = \int_0^1 f \left[ U'' - \frac{\alpha^2 r^2 - n^2}{r(\alpha^2 r^2 + n^2)} U' \right] \frac{|v|^2}{|U - c|^2} (U - c)^* dr \quad (A10)$$

where superscript  $*$  denotes complex conjugate. Integrating the first term in Eq. (A10) and applying the boundary conditions, we get

$$\int_0^1 (fv')' v^* dr = fv^* v'|_0^1 - \int_0^1 f |v'|^2 dr = - \int_0^1 f |v'|^2 dr \quad (A11)$$

Since  $f$  is always positive [see Eq. (A9)], the first and second terms in Eq. (A10) are real and negative. For any  $n \geq 1$  the third term is also zero or negative. For  $n=0$ , combination of the second and third terms in Eq. (A10) gives

$$\begin{aligned}
& - \int_0^1 f \left[ \frac{\alpha^2 r^2 + n^2 + 2}{\alpha^2 r^2 + n^2} \right] \alpha^2 |v|^2 dr + \int_0^1 f(1 - n^2) \frac{|v|^2}{r^2} dr \\
& = - \int_0^1 f \frac{|v|^2}{r^2} (1 + \alpha^2 r^2) dr \tag{A12}
\end{aligned}$$

This is also a negative quantity. Hence for any  $n$ , the left-hand side of Eq. (A10) is real and negative. Now the imaginary part of Eq. (A10) is

$$c_i \int_0^1 f \left[ U''' - \frac{(\alpha^2 r^2 - n^2)}{r(\alpha^2 r^2 + n^2)} U' \right] \frac{|v|^2}{|U - c|^2} dr = 0 \tag{A13}$$

where  $c_i$  is the imaginary part of the phase speed  $c$ . For flow to be unstable  $c_i > 0$ , hence

$$\int_0^1 f I \frac{|v|^2}{|U - c|^2} dr = 0 \tag{A14}$$

where

$$I \equiv U''' - \frac{(\alpha^2 r^2 - n^2)}{r(\alpha^2 r^2 + n^2)} U' \tag{A15}$$

Therefore a necessary condition of instability for pipe flow is the quantity  $I=0$  at some radial location in the domain. Setting  $r \rightarrow \infty$  in Eq. (A14), we recover Rayleigh's criterion for two-dimensional flow.

Now consider a flow where  $I$  undergoes a sign change in the profile. The real part of the Eq. (A10) is given by

$$\int_0^1 f(U - c_r) \left[ U''' - \frac{(\alpha^2 r^2 - n^2)}{r(\alpha^2 r^2 + n^2)} U' \right] \frac{|v|^2}{|U - c|^2} dr \leq 0 \tag{A16}$$

Multiplying Eq. (A14) with  $(c_r - U_s)$ , we get

$$\int_0^1 f(c_r - U_s) \left[ U''' - \frac{(\alpha^2 r^2 - n^2)}{r(\alpha^2 r^2 + n^2)} U' \right] \frac{|v|^2}{|U - c|^2} dr = 0 \tag{A17}$$

where  $U_s$  is the axial velocity at the radial location where  $I=0$ . Now adding Eqs. (A16) and (A17), we have

$$\int_0^1 f(U - U_s) \left[ U''' - \frac{(\alpha^2 r^2 - n^2)}{r(\alpha^2 r^2 + n^2)} U' \right] \frac{|v|^2}{|U - c|^2} dr \leq 0 \tag{A18}$$

which implies that for the flow to be unstable, we must have

$$(U - U_s) \left[ U''' - \frac{(\alpha^2 r^2 - n^2)}{r(\alpha^2 r^2 + n^2)} U' \right] \leq 0 \tag{A19}$$

This gives an additional necessary condition of instability for pipe flows. As discussed above the two-dimensional counterpart of the above criterion is known as Fj\o rtoft's theorem.

## References

- [1] Pearson, J. R. A., 1985, *Mechanics of Polymer Processing*. Elsevier, London.
- [2] Sukaneck, P. C., Goldstein, C. A., and Laurence, R. L., 1973, "The Stability of Plane Channel Flow With Viscous Heating," *Journal of Fluid Mechanics*, **57**, pp. 651–670.
- [3] Wylie, J. J., and Huang, H., 2007, "Extensional Flows With Viscous Heating," *Journal of Fluid Mechanics*, **571**, pp. 359–370.
- [4] Yueh, C. S., and Weng, C. I., 1996, "Linear Stability Analysis of Plane Couette Flow With Viscous Heating," *Physics of Fluids*, **8**(7), pp. 1802–1813.
- [5] White, J., and Muller, S., 2000, "Viscous Heating and the Stability of Newtonian and Viscoelastic Taylor-Couette Flows," *Physical Review Letters*, **84**, pp. 5130–5133.
- [6] Pinarbasi, A., and Imal, M., 2005, "Viscous Heating Effects on the Linear Stability of Poiseuille Flow of an Inelastic Fluid," *Journal of Non-Newtonian Fluid Mechanics*, **127**, pp. 61–71.
- [7] Costa, A., and Macedonio, G., 2005, "Viscous Heating Effects in Fluids With Temperature-Dependent Viscosity: Triggering of Secondary Flows," *Journal of Fluid Mechanics*, **540**, pp. 21–38.
- [8] Sahu, K. C., and Matar, O. K., 2010, "Stability of Plane Channel Flow With Viscous Heating," *ASME Journal of Fluids Engineering*, **132**, p. 011202.
- [9] Swaminathan, G., Sahu, K. C., Sameen, A., and Govindarajan, R., 2011, *Theoretical and Computational Fluid Dynamics*, **25**(1–4), pp. 53–64.
- [10] Floryan, J. M., and Floryan, C., 2010, "Traveling Wave Instability in a Diverging-Converging Channel," *Fluid Dynamics Research*, **42**(2), p. 025509.
- [11] Sahu, K. C., and Govindarajan, R., 2005, "Stability of Flow Through a Slowly Diverging Pipe," *Journal of Fluid Mechanics*, **531**, pp. 325–334.
- [12] Drazin, P. G., 1999, "Flow Through a Diverging Channel: Instability and Bifurcation," *Fluid Dynamics Research*, **24**(6), pp. 321–327.
- [13] Selvarajan, S., Tulapurkara, E. G., and Ram, V. V., 1999, "Stability Characteristics of Wavy Walled Channel Flows," *Physics of Fluids*, **11**(3), pp. 579–590.
- [14] Peixinho, J., 2010, "Flow in a Slowly Divergent Pipe Section," *Seventh IUTAM Symposium on Laminar-Turbulent Transition*, **18**(2), pp. 307–312.
- [15] Davis, S. H., Kriegsmann, G. A., Laurence, R. L., and Rosenblat, S., 1983, "Multiple Solutions and Hysteresis in Steady Parallel Viscous Flows," *Physics of Fluids*, **26**(5), pp. 1177–1182.
- [16] Eldabe, N. T. M., El-Sabbagh, M. F., and El-Sayed(Hajjaj), M. A.-S., 2007, "The Stability of Plane Couette Flow of a Power-Law Fluid With Viscous Heating," *Physics of Fluids*, **19**, p. 094107.
- [17] Ho, T. C., Denn, M. M., and Anshus, B. E., 1977, "Stability of Low Reynolds Number Flow With Viscous Heating," *Rheology Acta*, **16**, pp. 61–68.
- [18] Becker, L. E., and McKinley, G. H., 2000, "The Stability of Viscoelastic Creeping Plane Shear Flows With Viscous Heating," *Journal of Non-Newtonian Fluid Mechanics*, **92**, pp. 109–133.
- [19] Nahme, R., 1940, "Beiträge zur Hydrodynamischen Theorie der Lagerreibung," *Ingenieur-Archiv*, **11**, pp. 191–209.
- [20] Pinarbasi, A., and Ozalp, C., 2001, "Effect of Viscosity Models on the Stability of a Non-Newtonian Fluid in a Channel With Heat Transfer," *International Committee on Heat Mass Transfer*, **28**(3), pp. 369–378.
- [21] Rayleigh, L., 1880, "On the Stability of Certain Fluid Motions," *Proceedings of the London Mathematical Society*, **11**, pp. 57–70.
- [22] Bertolotti, F. P., Herbert, T., and Spalart, P. R., 1992, "Linear and Nonlinear Stability of the Blasius Boundary Layer," *Journal of Fluid Mechanics*, **242**, pp. 441–474.
- [23] Bird, R. B., Stewart, W. R., and Lightfoot, E. N., 2002, *Transport Phenomena*, John Wiley & Sons, New York.
- [24] Gill, A. E., 1973, "The Least-Damped Disturbance to Poiseuille Flow in a Circular Pipe," *Journal of Fluid Mechanics*, **61**, pp. 97–107.
- [25] Lessen, M., Sadler, S. G., and Liu, T. Y., 1968, "Stability of Pipe Poiseuille Flow," *Physics of Fluids*, **11**, pp. 1404–1409.
- [26] Batchelor, G. K., and Gill, A. E., 1962, "Analysis of the Stability of Axisymmetric Jets," *Journal of Fluid Mechanics*, **14**, pp. 529–551.
- [27] Canuto, C., Hussaini, M. Y., Quarteroni, A., and Zang, T., 1987, *Spectral Methods in Fluid Dynamics*, 1st ed., Springer, Amsterdam.
- [28] Schmid, P. J., and Henningson, D. S., 2001, *Stability and Transition in Shear Flows*, Springer, New York.
- [29] Burridge, D. M., and Drazin, P. G., 1969, "Comments on Stability of Pipe Poiseuille Flow," *Physics of Fluids*, **12**, pp. 264–265.
- [30] Corcos, G. M., and Sellars, J. R., 1959, "On the Stability of Fully Developed Flow in a Pipe," *Journal of Fluid Mechanics*, **5**, pp. 97–112.
- [31] Selvam, B., Merk, S., Govindarajan, R., and Meiburg, E., 2007, "Stability of Miscible Core-Annular Flows With Viscosity Stratification," *Journal of Fluid Mechanics*, **592**, pp. 23–49.
- [32] Rayleigh, L., 1880, "On the Stability of Certain Fluid Motions," *Proceedings of the London Mathematical Society*, **11**, pp. 57–70.
- [33] Sameen, A., and Govindarajan, R., 2007, "The Effect of Wall Heating on Instability of Channel Flow," *Journal of Fluid Mechanics*, **577**, pp. 417–442.
- [34] Fj\o rtoft, R., 1950, "Application of Integral Theorems in Deriving Criteria of Stability for Laminar Flows and for the Baroclinic Circular Vortex," *Geofysics Publications of Oslo*, **17**(6), pp. 1–52.
- [35] Sahu, K. C., 2007, "Novel Stability Problems in Pipe Flows," Ph.D. thesis, Jawaharlal Nehru Centre for Advanced Scientific Research, Bangalore, India, Bangalore, India.